CHAPTER II

ONE-POT SYNTHESIS AND CHARACTERIZATION OF NOVEL SODIUM TRIS(GLYCOZIRCONATE) AND CERIUM GLYCOLATE PRECURSORS AND THEIR PYROLYSIS

Abstract

A low-cost and facile route to the synthesis of bimetallic glycolato zirconate ($Na_2Zr(C_2H_4O_2)_3$) and homometallic glycolato cerate ($Ce(C_2H_4O_2)$), which can be used as alkoxide precursors for sodium zirconium oxide (and/or zirconia by sol-gel process) and ceria materials, has been developed from the reaction of inexpensive starting materials via the oxide one pot synthesis (OOPS) process. Both complexes were directly synthesized from zirconium hydroxide/cerium hydroxide and ethylene glycol using base as catalyst. Sodium hydroxide was used in the synthesis of sodium tris(glycozirconate) complex while both triethylenetetramine (TETA) as catalyst and trace amount of sodium hydroxide as co-catalyst were used in the case of cerium glycolate complex. The structures of obtained products were investigated using FTIR, TGA, DSC, ^{1}H- and ^{13}C-NMR, elemental analyses, EDS and mass spectroscopy. Pyrolysis studies delineate the effects of temperature on the decomposition processes whereby sodium tris(glycozirconate) and cerium glycolate precursors transform into $Na_2O.ZrO_2$ and CeO_2, respectively. The resulting sodium zirconium oxide and ceria, after pyrolysis at 600°C for 3 h, had BET surface areas of about 62 and 70 $m^2\ g^{-1}$, respectively, and show monomodal pore size distributions in the mesopore region.

Introduction

Intense interest has been focused on the investigation of novel metal alkoxides during the last two decades owing to their use as precursors in the sol-gel synthesis of inorganic metal oxides for catalytic, composite, and electroceramic materials, coatings and fibers.[1-5] Simple metal alkoxides $M(OR)_n$ with usual OR ligands are commercially available for a large number of metals. However, some significant drawbacks of simple metal alkoxides make it difficult to investigate their structures. These are their relatively high cost and low hydrolytic stability or high reactivity towards water.[6,7] Their high reactivity is the main problem in processing inorganic oxides from alkoxides by sol-gel method. Many researchers have resolved these problems by modifying the simple alkoxide precursors to reduce hydrolytic reactivity in order to avoid a precipitate formation.[8-10] The general approach is to replace one or more alkoxide ligands by groups which are less easily hydrolyzed and additionally block coordination sites at the metal. However, the modifications are rather complicated and expensive. The synthesis of new metal alkoxides possessing unique structures and properties is important for the study of sol-gel processes and the evolution of metal alkoxide chemistry.

Anodic dissolution of the metal can provide an easy and straightforward way to scale up synthesis of alkoxides for many metals.[11] Reactions between oxides or hydroxides and dialkylcarbonates, polyols or aminoalcohols can also be cost-effective routes to new metal alkoxides of some elements.[12-13] This route is termed as the 'oxide one-pot synthesis' (OOPS) process. Most of work on this area of research has been done on Si, Al, and Ti metals with the chelate diol.[14-22] Interestingly, metal derivatives of glycol are comparatively more hydrolytic resistant than their alkoxide analogues. The chelating nature of the glycol and coordinative saturation achieved by the central atoms in the final products appear to be the main factor for their hydrolytic stability to retard the hydrolysis and condensation reaction rates in order to obtain homogeneous gels rather than precipitates.[10]

Sodium zirconium oxide is one of inorganic ion exchange materials having high affinity for all actinides and fission product cations in fast breeder reactors.[23-24] Zirconia materials have a wide range of applications including catalytic supports,

composites, absorbates, and optical, electronic, magnetic and thermal fields.[25-27] Ceria is currently being used as a promoter or support in several industrial catalytic processes and as a key component in the formulation of catalysts for automotive emission control. The most important role of ceria in this application is to act as an oxygen storage material. This property is known to widen the operational window for the automotive catalytic converters.[28-30] In the last decade, it also was shown that the addition of zirconium into the ceria lattice could improve thermal resistance and durability of automotive catalysts. Thus, ceria-zirconia materials are of interest in the application of three-way catalysts.[31-33]

In this research, we extend the efforts to synthesize other transition metalloglycolates so as to be further used as metal alkoxide precursors in the sol-gel study. We investigate the synthesis of zirconium and cerium glycolate complexes, which will be used further as precursors for high surface area zirconia and ceria by sol-gel processes. In this present work, we also study the thermal decomposition of both synthesized precursors. The syntheses are carried out using the OOPS process from the reaction of inexpensive and easily available starting materials, ethylene glycol and zirconium or cerium hydroxide, as compared to metal alkoxides which are commonly used and far more expensive. These obtained alkoxide precursors containing ethylene glycolate ligands are hydrolytically stable, thus yielding more controllable chemistry and minimizing special handling requirement.

Experimental Section

Materials. The starting materials were slightly either moisture or air sensitive. Therefore, all glassware used in these experiments was dried in an oven at 110°C overnight. All syntheses were carried out with careful exclusion of extraneous moisture by purging under an atmosphere of nitrogen.

UHP grade nitrogen (99.99% purity) was obtained from Thai Industrial Gases Public Company Limited (TIG). Zirconium (IV) hydroxide ($Zr(OH)_4$) containing 88.8% ZrO_2 and cerium(IV) hydroxide ($Ce(OH)_4$) containing 87.4% CeO_2 as determined by TGA were purchased from Aldrich Chemical Co. Inc. (USA) and used as received. Ethylene glycol (EG), purchased from Farmitalia Carlo Erba

(Barcelona), was purified by fractional distillation under nitrogen at atmospheric pressure, 200°C before use. Sodium hydroxide was purchased from Merck Company Co. Ltd. (Germany) and used as received. Triethylenetetramine (TETA) was purchased from Facai Polytech. Co. Ltd. (Bangkok, Thailand) and distilled under vacuum (0.1 mmHg) at 130°C prior to use. Methanol and acetonitrile were purchased from Lab-Scan Company Co. Ltd. and purified by standard techniques. Methanol was distilled over magnesium activated with iodine. Acetonitrile was distilled over calcium hydride powder.

Instruments. FTIR spectra were recorded on a Vector3.0 Bruker spectrometer with a spectral resolution of 4 cm^{-1} using transparent KBr pellet. The samples were thoroughly crushed and mixed with KBr at an approximate ratio by weight of sample:KBr of 1: 20. Thermogravimetric analyses (TGA) were carried out in a TGA7 Perkin Elmer thermal analysis system with a heating rate of 10°C min^{-1} over a 25-800°C temperature range. Differential Scanning Calorimetry (DSC) analyses were conducted on a Netzsch DSC 200 (Germany) from 25 to 500° C at the heating rate of 10° C min^{-1}. ^{1}H- and ^{13}C-NMR spectra were obtained on a Bruker 200 MHz spectrometer at the Chemistry Department, Faculty of Science, Chulalongkorn University, using deuterated dimethyl sulfoxide (DMSO-d_6) as solvent and reference for chemical shift measurements at room temperature. Variable temperature NMR spectra were examined on a JEOL 500 MHz spectrometer in the temperature range 25–140°C. Mass spectra were recorded on both FAB and ion trap modes. The positive fast atom bombardment mass spectrometer (FAB^{+}-MS) was a Fison Instrument (VG Autospec-ultima 707E) with VG data system using glycerol as the matrix, cesium gun as initiator, and cesium iodide (CsI) as a standard for peak calibration. Liquid chromatography mass spectrometer (LC-MS) was a Bruker Esquire-LC using methanol as a mobile phase. A JEOL Model 5200 scanning electron microscope equipped with EDS system was employed for X-ray microanalysis. After pyrolysis, textural characterization of the as-synthesized products was performed on an Autosorb-1 gas sorption system (Quantachrome Corp.). The BET surface area, pore volume, and pore size

distribution of the pyrolyzed products were obtained from nitrogen adsorption-desorption at 77 K. Powder X-ray diffraction (XRD) patterns were obtained using a Rigaku D/Max diffractrometer consisting Cu Kα radiation (λ=0.154 nm).

Syntheses

Preparation of sodium tris(glycozirconate) complex ($Na_2Zr(C_2H_4O_2)_3$). A mixture of zirconium hydroxide (1.59 g, 11.4 mmol of ZrO_2) and approximate 200 mol % sodium hydroxide equivalent to zirconium dioxide were suspended in 35 ml of ethylene glycol (EG). The reaction mixture was heated under nitrogen in a thermostatted oil bath. When the thermostatted oil bath reached the boiling point of ethylene glycol, the reaction was considered to have commenced. Ethylene glycol was slowly distilled off so as to remove any liberated water from the reaction. After 12 h the solution was virtually clear, indicating reaction completion. The reaction mixture was cooled, and a 2-5% of dried methanol in acetonitrile was added. The product precipitated out as a white solid. The solid was filtered off, washed with acetonitrile (3 x 15 ml) and dried under vacuum (0.1 mmHg) at room temperature.

Preparation of cerium glycolate complex, $Ce(C_2H_4O_2)_2$. A mixture of cerium hydroxide (1.04 g, 5.3 mmol of CeO_2), 18 ml of ethylene glycol and 5 mmol (0.73 g) triethylenetetramine with sodium hydroxide at about 12 mol% equivalent to cerium hydroxide was magnetically stirred and heated to the boiling point of ethylene glycol for 18 h under nitrogen to distill off ethylene glycol with removal of water liberated from the reaction. The reaction mixture was cooled overnight under nitrogen. The precipitated product was filtered and washed with acetonitrile (3 x 15 ml), followed by drying under vacuum, as described above.

Results and Discussion

Synthesis. The reaction of zirconium hydroxide, ethylene glycol and sodium hydroxide was obtained by heating the reaction mixture in a magnetically stirred, standard pyrex distillation setup and slowly distilling off the excess ethylene glycol

under nitrogen at atmospheric pressure to immediately remove by-product, water, formed from the reaction. In the case of cerium hydroxide reacting with ethylene glycol, the reaction occurs faster and does not need a base as strong as zirconium hydroxide. Triethylenetetramine was employed as catalyst with a small amount of sodium hydroxide as co-catalyst to achieve the desired product. In both reactions, ethylene glycol served not only as a solvent but also as a reactant, forming two and three bidentate chelates for cerium and zirconium hydroxides, respectively. This is the reason why an excess ethylene glycol, distilled off with removal of water, was essential to achieve the high percentage yields of the products. Both products provided powders at approximately 90% isolated yields. The products were isolated by addition of dried acetonitrile to the solution to result in white and yellow-green solids for sodium tris(glycozirconate) and cerium glycolate complexes, respectively. Repeated washing with dried acetonitrile was necessary to remove residual TETA and ethylene glycol. The series of reactions for synthesizing, sodium tris(glycozirconate) and cerium glycolate complexes were thus prepared as illustrated in Scheme 1.

Characterization. FTIR, TGA, DSC, ^{1}H- and ^{13}C-NMR, elemental analyses, EDS and MS were used to investigate the structure of zirconium and cerium glycolate complex products. The FTIR spectra of both products and their starting materials are given in Figs. 1 and 2. The bands located at 2939 and 2873 cm^{-1} were assigned to the ν(C-H) stretching frequency. The C-H deformation vibrations were attributed to the band in the region of 1400-1200 cm^{-1} of methylene groups. Sodium tris(glycozirconate) complex displayed the band at 1090 cm^{-1}, corresponding to the Zr-O-C stretching vibration mode, and 880 cm^{-1} indicating to the deformation vibration of the C-C bond. An additional band occurring at around 613 cm^{-1} was assigned to the Zr-O stretching frequency.[34-36] As for cerium glycolate complex, the resonance at 1080 cm^{-1} was ascribed to the Ce-O-C stretching vibration, and the band at 550 cm^{-1} is from the Ce-O stretching.[37-38] FT-IR spectra not only show the major bands of both products, but also indicate their moisture absorption. On exposure to the atmosphere during pellet preparation, the products show the OH bands at 3700-

3000 and 1600 cm^{-1} corresponding to the O-H stretching and the bending vibrations of water absorbed from the moisture in the air. It is worth noting that these two bands in zirconium glycolate complex spectrum are broader than those in cerium glycolate complex product. This is due to the more moisture sensitivity of zirconium glycolate complex attributed to the presence of the sodium salt in its structure. The reason became clearer when the mass spectroscopy and EDS results showed the actual structure of zirconium glycolate complex as sodium salt.

The thermal behavior of both products was investigated by means of TGA and DSC measurements. The TGA traces can be used to confirm the composition of the proposed products. The TG and derivative TG (DTG) profiles of sodium tris(glycozirconate) complex (Fig. 3) show one major thermal decomposition ranging from 350 to 545 °C. Its weight loss of 41.59 % corresponded to conversion of as-synthesized product into carbon-free inorganic materials or to the decomposition of all organic ligands from the product framework. This experimental weight loss is consistent with the theoretical weight loss calculated for the formation of the proposed product $Na_2O.ZrO_2$, which was 41.67 %. The percentage ceramic yield of the product was 58.41 %, which in excellent agreement with the theoretical value (58.33%). In addition, EDS can be used to confirm the formation of $Na_2O.ZrO_2$ after thermal decomposition. The resulting Na/Zr ratio equals to 1.98, which is consistent with the proposed oxide product (2.0).

Similarly, the TG and DTG thermograms of cerium glycolate complex, given in Fig. 4, also exhibit one transition at around 350 - 525°C. The weight loss (34.1%) is due to the total breakdown of the organic species, resulting in the metal oxide CeO_2. The product gave a ceramic yield of 65.9% in agreement with the calculated yield 66.1%.

The weight loss of sodium tris(glycozirconate) complex is higher than that of cerium glycolate complex. This is due to the higher number of ethylene glycolate ligands contained in its structure.

The DSC traces of sodium tris(glycozirconate) and cerium glycolate complexes display an exotherm at 430 and 410°C, respectively. These results are in agreement with the TGA results.

The ^{1}H- and ^{13}C-NMR spectra of both products were recorded in deuterated DMSO. It can be seen that ^{1}H-NMR spectra attributed to the as-synthesized products shows only one singlet peak at 3.3 and 3.4 ppm for sodium tris(glycozirconate) and cerium glycolate complexes, respectively. They are assigned to chelated glycolate ligands of CH_2-O-Zr and CH_2-O-Ce.

Similarly, the ^{13}C-NMR spectra display a single peak at 62.6 and 62.8 ppm for sodium tris(glycozirconate) and cerium glycolate complexes, respectively. They belong to the symmetrical carbons of chelated glycolate ligands (CH_2-O-Zr, CH_2-O-Ce). These compounds are highly pure materials and not solvated with free ethylene glycol molecules due to no signals at 3.6, 4.3 and 63.9 ppm in ^{1}H- and ^{13}C-NMR spectra, respectively. This observation is also consistent with the TGA and DSC results.

Using elemental analyzer to confirm the synthesized products, it was found that the obtained percentages of carbon and hydrogen are very close to those theoretically calculated. For sodium tris(glycozirconate) precursor, anal. calcd. (%): C, 22.70; and H, 3.78 and found (%): C, 22.41; and H, 4.23. For cerium glycolate complex, anal. calcd. (%): C, 18.45; and H, 3.08 (3.42) and found (%): C, 18.28; and H, 3.08. Nevertheless, the Na/Zr atomic ratio of sodium tris(glycozirconate) precursor observed by EDS was 1.97 corresponding to the calculated ratio (2.0).

The MS spectrum fragmentation pattern can be employed to explain the basis of the proposed product structure and to confirm the proposed structures, as summarized in Tables 1 and 2 for sodium tris(glycozirconate) and cerium glycolate precursors, respectively. According to the obtained fragmentation patterns, the expected products were successfully synthesized.

Generally, the product can be either a coordination hydrate or an oligomeric species. Mass spectral analysis of the crude form of sodium tris(glycozirconate) and cerium glycolate complexes was also employed to determine the molecular complexities of these crude products. The results suggest that the mass species is consistent with the dimeric and trimeric structures for sodium tris(glycozirconate) and cerium glycolate complexes, respectively (Tables 1 and 2). After purification of these crude products in acetronitrile, the mass spectra of purified form appeared to be

monomeric species. The proposed monomeric behavior of both purified products was confirmed by variable temperature NMR spectra (Fig. 5(a) and (b)) in DMSO-d_6 solution indicating one signal due to chelated glycolate ligands independent of temperature. As a result of these experiments, it is probably implied that the crude oligomeric products dissociate to the monomeric form during purification. In the case of cerium glycolate complex, cerium metal exhibits coordination of 4. Coincidently, Bradley *et al.*[39] also showed that for the secondary alkoxides the cerium is predominantly six-coordinated in boiling benzene with only a small percentage in the eight-coordinated state, whilst it appears that further dissociation of the trimeric molecules to the monomeric four-coordinated state. Reasonably, it could be implied that in our purified product the cerium metal is four-coordinated, and the monomeric structure containing only two bidentate glycols was obtained. No oligomeric species was observed despite the obvious opportunity to form.

Precursor Pyrolysis Study. A one-stage pyrolysis process based on the TGA and DSC traces was used to pyrolyze these as-synthesized precursors. Upon decomposition of the organic ligands in the temperature range discussed in the thermal analysis part, the precursors were heated to 500, 600, 700 and 800°C with a rate of 10°C min^{-1} for 3 h. The XRD patterns of sodium tris(glycozirconate) and cerium glycolate precursors are shown in Figs. 6 and 7, respectively. At the temperature 500°C, the pyrolyzed sodium tris(glycozirconate) precursor exhibits a grayish appearance due to residual carbon. Upon further increasing the pyrolysis temperature, the XRD pattern of sodium zirconium oxide was observed. The increasing sharpness and intensity of the powder pattern were much enhanced. The cerium glycolate precursor generated a broad peak for CeO_2 after heated at 500°C. The crystallinity was gradually increased with increasing pyrolysis temperature.

BET surface area for sodium tris(glycozirconate) and cerium glycolate precursors obtained after thermal treatment at increasing temperatures are reported in Figs. 8(a) and (b), respectively. All powders show a decrease of the surface area with increasing pyrolysis temperature due to sintering. This is also in agreement with the narrow diffraction peaks, indicating the crystallite growth. The exceptional

surface area at 500°C was attributed to free carbon remaining in the sample, indicating a need for higher pyrolysis temperature. The nitrogen adsorption/desorption isotherms for the pyrolyzed sodium tris(glycozirconate) and cerium glycolate precursors at 600°C are presented in Figs. 9(a) and 10(a), respectively. Both powders show isotherms of type IV (IUPAC classification) which exhibit hysteresis loops mostly of type H2.[40]

This indicates that the powders contain mesopores. Also, the isotherms show one hysteresis loop, indicating monomodal pore size distributions, as shown in Figs. 9(b) and 10(b). The pore size distribution in the mesopore range had a maximum center around a pore diameter of 70 and 60 Å for the pyrolyzed sodium tris(glycozirconate) and cerium glycolate precursors, respectively. This monomodal pore size distribution was observed probably due to the highly pure precursors. This is also in agreement with the thermal analysis results mentioned above, where all weight loss was detected in one step. The decomposition of all organic ligands from the product framework was observed between 350 and 550 °C.

Some approaches that have been recently applied to prepare ceria powder are precipitation techniques[41-42], microemulsion[43], spray pyrolysis methods[44], electrochemical methods[45], hydrothermal synthesis[46], and thermal decomposition of carbonates[47]. In most cases, ceria was reported with the surface area less than 100 $m^2 g^{-1}$ at the temperature lower than 500°C. Generally, a loss of surface area is caused by thermal treatment. In our case, surface area approximately 100 $m^2 g^{-1}$ was obtained after pyrolysis at 500°C. Although, the direct pyrolysis method can be used for the preparation of sodium zirconium oxide and ceria materials, thermal stability of both oxide products is rather poor. In forthcoming papers, the preparation of higher surface area zirconia, ceria, and ceria-zirconia materials from both novel synthesized alkoxide precursors via sol-gel route will be discussed in detail.

Conclusions

We have successfully synthesized the chelated metal alkoxide precursors, zirconium and cerium glycolate complexes, using the "oxide one pot synthesis process" in very high yields. The ethylene glycol is used as solvent as well as a

reactant material. We have also showed a simple way to convert sodium tris(glycozirconate) and cerium glycolate precursors to sodium zirconium oxide and ceria by direct pyrolysis without going through other processes. However, this direct pyrolysis technique limits control of the microstructure and surface features obtained. To obtain a higher surface area and a wider range of the pore sizes, the effect of various factors governing the sol-gel routes on the resulting structural properties has been investigated to compare with the direct pyrolysis method.

Acknowledgments

This work was fully funded by the Thailand Research Fund. The authors are grateful to ADB Fund, Ratchadapisake Sompote Fund, Chulalongkorn Univerisity, and The Chemistry Department, Chulalongkorn University, for supporting equipment and conducting ^{1}H- and ^{13}C-NMR spectra, respectively.

References

1. Bradley, D.C.; Mehrotra, R.C.; Gaur, D.P. *Metal Alkoxides*; Academic Press: New York, **1978**.
2. Brinker, C.J.; Scherer, G.W., *Sol-Gel Science: The Physics and Chemistry of Sol-Gel Processing*; Academic Press: San Diego, 1990.
3. Jones, R.W., *Fundamental Principles of Sol-Gel Technology*; The Institute of Metals: London, 1989.
4. Hench, L.L.; West, J.K., *Chem. Rev.*, **1990**, *90*, 33.
5. Klein, L.C., *Sol-Gel Technology for Thin Films, Fibers, Performs, Electronics, and Speciality Shapes*; New Jersey, 1988.
6. Huling, J.C.; Messing, G.L., *J. Non-Cryst. Solids*, **1992**, *147&148*, 213.
7. Schneider, H.; Saruhan, B.; Voll, D.; Merwin, L.; Sevald, A., *J. Eur. Ceram. Soc.*, **1993**, *11*, 87.
8. Guizard, C.; Cygankiewcz, N.; Larbot, A.; Cot, L., *J. Non-Cryst. Solids*, **1986**, *82*, 86.
9. Debsikdar, J.C., *J. Non-Cryst. Solids*, **1986**, *86*, 231.
10. Mehrotra, R.C.; Anirudh Singh. *Prog. Inorg. Chem.*, **1997**, *46*, 239.

11. Turevskaya, E.P.; Kozlova, N.; Shreider, V.; Ya Turova N., *Inorg. Chim. Acta.*, **1981**, *53*, 573.
12. Suzuki, E.; Kusano, S.; Hatayama, H.; Okamoto, M.; Ono, Y., *Chem. Mater.*, **1997**, *7*, 2049.
13. Kemmitt, T.; Al-Salim, N.I; Gainsford, G.J.; Henderson, W., *Aust. J. Chem.*, **1999**, 52, 10915.
14. Laine, R.M.; Blohowiak, K.Y. ; Robinson, T.R.; Hoppe, M.L.; Nardi, P.; Kampf, J.; Uhm, J., *Nature* **1991**, *353*, 642.
15. Blohowiak, K.Y; Laine, R.M.; Robinson, T.R.; Hope, M,L.; Kampf, J.I., *Inorganic and Organometallic Polymers with Special Properites*; ACS: Netherlands, 1992.
16. Bickmore, C.; Hoppe, M.L.; Laine, R.M., *Mat .Res. Soc. Symp. Proc.*, **1992**, *249*, 81.
17. Jitchum, V.; Chivin, S.; Wongkasemjit, S.; Ishida, H., *Tetrahedron,* **2001**, *57*, 3997.
18. Laine, R.M.; Youngdahl, K.A.; Nardi, P. Washington Research Foundation, U.S. Pat. No.5,099,052, 1992.
19. Laine, R.M.; Youngdahl, K.A. Washington Research Foundation, U.S. Pat. No. 5,216,155, 1993.
20. Gainsford, G.J.; Kemmitt, T.; Milestone, N.B., *Inorg. Chem.* **1995**, *34*, 5244.
21. Gainsford, G.J.; Kemmitt, T.; Lensink, C.; Milestone, N.B., *Inorg. Chem.,* **1995**, *34*, 746.
22. Wang, D.; Yu, R.; Kumada, N.; Kinomura, N., *Chem. Mater.,* **1999**, *11*, 2008.
23. Kenna. B.T.; Murphy. K.D., *J. Inorg. Nucl. Chem.,* **1979**, *41*, 1535.
24. Subasri, R.; Mathews, T.; Swaminathan. K.; Sreedharan, O.M., *J. Nucl. Mater.* **,2002**, *300*, 237.
25. Hsiao-Lan, C.; Phillip, S.; Wei-Heng, S., *J. Am. Ceram. Soc.*, **2000**, *83*, 2055.
26. Junping, Z.; Wenhao, F.; Dong, W.; Yuhan, S., *J. Non-Cryst. Solids,* **2000**, *261*, 15.
27. Narula, C.K.; Allison, J.E.; Bauer, D.R.; Gandhi, H.S., *Chem.Mater.*, **1996**, *8*, 984.

28. Powell, B.R.; Bloink, R.L.; Eickel. C.C., *J. Am. Ceram. Soc.*, **1988**, *71*, 104.

29. Trovarelli, A. *Catal. Rev.-Sci. Eng.*, **1996**, *38*, 439.

30. Kaspar.J.; Fornasiero, P.; Graziani, M., *Catal. Today,* **1999**, *50*, 285.

31. Ozawa, M. *J., Alloys Compd.*, **1998**, *275-277*, 886.

32. Masui, T.; Ozaki, T.; Machida, K.; Adachi, G.Y., *J. Alloys Compd.*, **2000**, *303-304*, 49.

33. Hori, C.E.; Permana, H.; Ng. K.Y.S.; Brenner, A.; Rahmoeller, K.M. Belton, D.N., Appl. Catal. B:Environ, **1998**, *16*, 105.

34. Colomban, P.; Bruneton, E., *J. Non-Cryst. Solids,* **1992**, *147&148*, 201.

35. Zhao, J.; Fan, W.; Wu, D.; Sun, Y., *J. Non-Cryst. Solids,* **2000**, *261*, 15.

36. He, T.; Jiao, X.; Chen, D.; Lu, M.; Yuan, D.; Xu, D., *J. Non-Cryst. Solids,* **2001**, *283*, 56.

37. Finocchio, E.; Daturi, M.; Binet, C.; Lavalley, J.C.; Blanchard, G., *Catal. Today,* **1999**, *52*, 53.

38. Holmgren, A.; Andersson, B.; Duprez, D. *Appl. Catal. B: Environ.*, **1999**, *22*, 215.

39. Bradley, D.C.; Chatterjee, A.K.; Wardlaw, W., *J. Chem. Soc.*, **1956**, 3469.

40. Leofanti, G.; Padovan, M.; Tozzola, G.; Venturelli, B., *Catal. Today,* **1998**, *41*, 207.

41. Abi-add, E.;Bechara, R.; Grimblot, J.; Aboukais, A., *Chem. Mater.*, **1993**, *5*, 793.

42. Bruce, L.A.; Hoang, M.; Hughes, A.E.; Turney, T.W.; *Appl. Catal. A: General* , **1996**, *134*, 351.

43. Matsui, T.; Fujiwara, K.; Machida, K.; Adachi, G.; Sakata, T.; Mori, H., *Chem. Mater.*, **1997**, *9*, 2197.

44. Vallet, R.M.; Conde, F.; Nicolopoulous, S.; Ragel, C.V.; Gonzales-Calbet, J.M., *Mater. Sci. Forum.,* **1997**, *235-238*, 291.

45. Zhou, Y.; Phillips, R.J.; Switzer, J.A., *J. Am. Ceram. Soc.*, **1995**, *78*, 981.

46. Hirano, M.; Kato, E., *J. Am. Ceram. Soc.*, **1996**, *79*, 777.

47. Pijalot, M.; Viricelle, J.P.; Soustelle, M., *Stud. Surf. Sci Catal.*, **1995**, *91*, 885.

Figure Captions

Figure 1. FTIR spectra of (a) sodium tris(glycozirconate) complex; (b) ethylene glycol;(c) $Zr(OH)_4$.

Figure 2. FTIR spectra of (a) cerium glycolate complex; (b) ethylene glycol; (c) $Ce(OH)_4$.

Figure 3. TG-DTG thermograms of sodium tris(glycozirconate) complex.

Figure 4. TG-DTG thermograms of cerium glycolate complex.

Figure 5. Variable temperature NMR spectra of (a) sodium glycozirconate complex; (b) cerium glycolate complex.

Figure 6. XRD patterns of sodium tris(glycozirconate) precursor at various pyrolysis temperatures. (a) $Na_2Zr(C_2H_4O_2)_3$ precursor; (b) 500°C; (c) 600°C; (d) 700°C; (e) 800°C. The reflections are according to Na_2ZrO_3 (ICDD no. 21-1179).

Figure 7. XRD patterns of cerium glycolate precursor at various pyrolysis temperatures. (a) $Ce(C_2H_4O_2)_2$ precursor; (b) 500°C; (c) 600°C; (d) 700°C; (e) 800°C. The reflections are according to CeO_2 (ICDD no. 43-1002).

Figure 8. Surface area versus pyrolysis temperature for (a) sodium tris(glycozirconate) precursor; (b) cerium glycolate precursor.

Figure 9. (a) Nitrogen adsorption/desorption isotherms; (b) Pore size distribution of sodium tris(glycozirconate) precursor pyrolyzed at 600°C for 3 h.

Figure 10. (a) Nitrogen adsorption/desorption isotherms; (b) Pore size distribution of cerium glycolate precursor pyrolyzed at 600°C for 3 h.

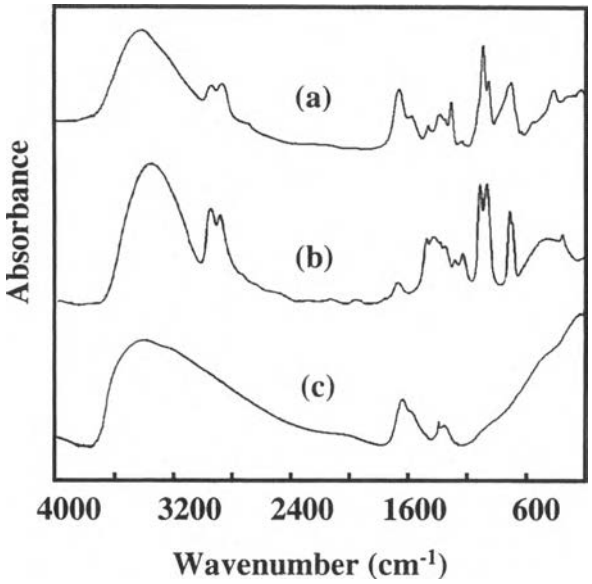

Figure 1. (Ksapabutr et al.)

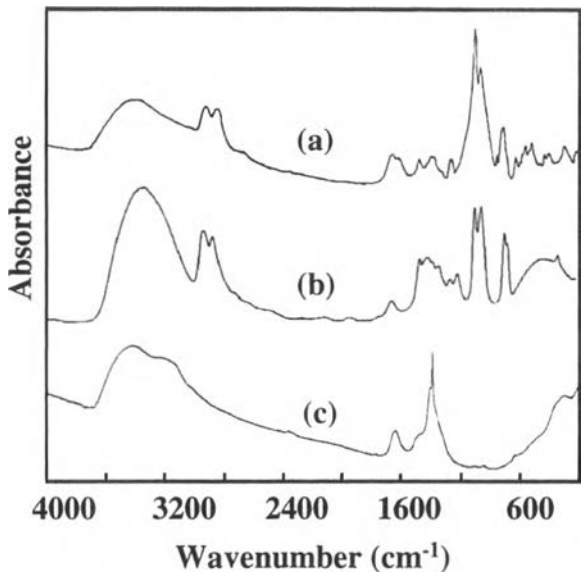

Figure 2. (Ksapabutr et al.)

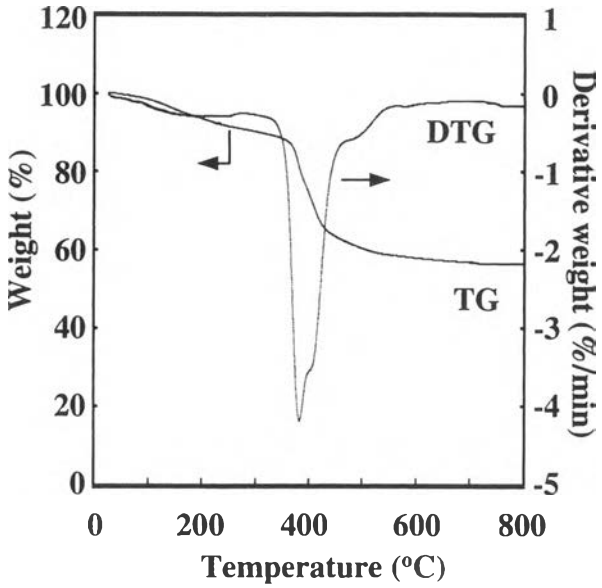

Figure 3. (Ksapabutr et al.)

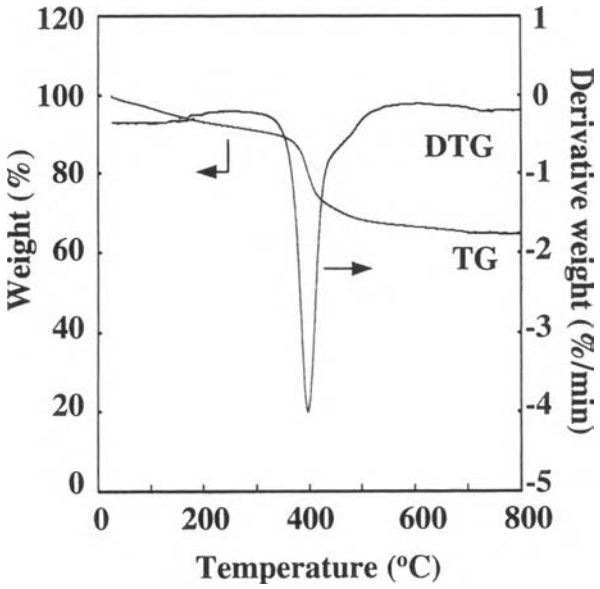

Figure 4. (Ksapabutr et al.)

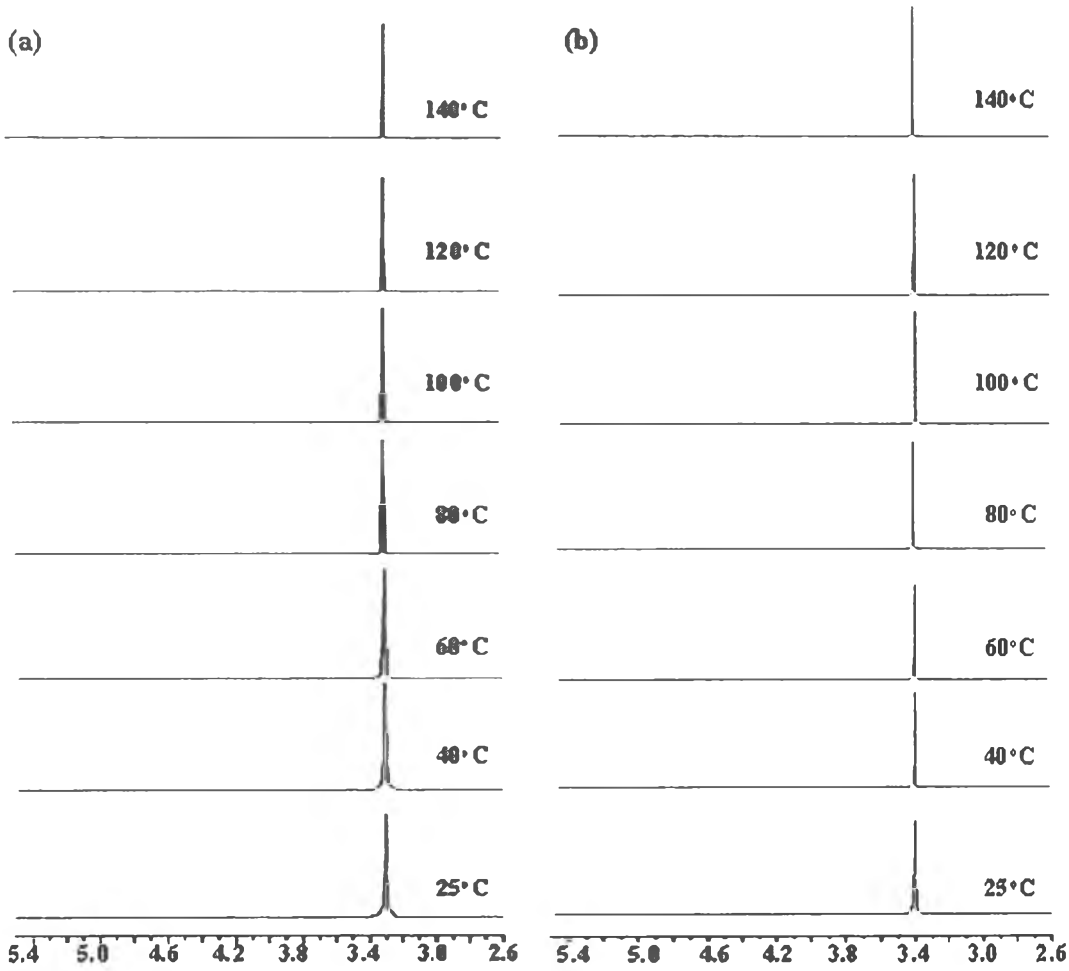

Figure 5. (Ksapabutr et al.)

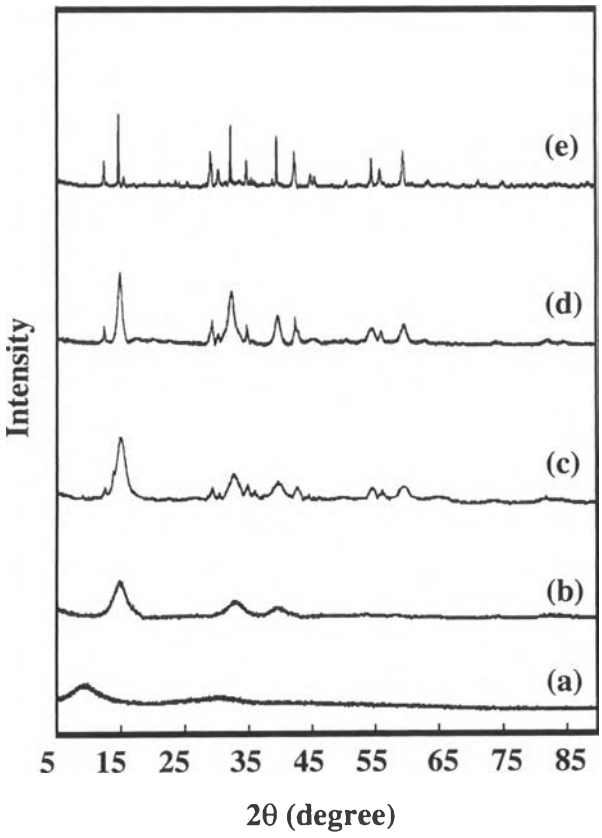

Figure 6. (Ksapabutr et al.)

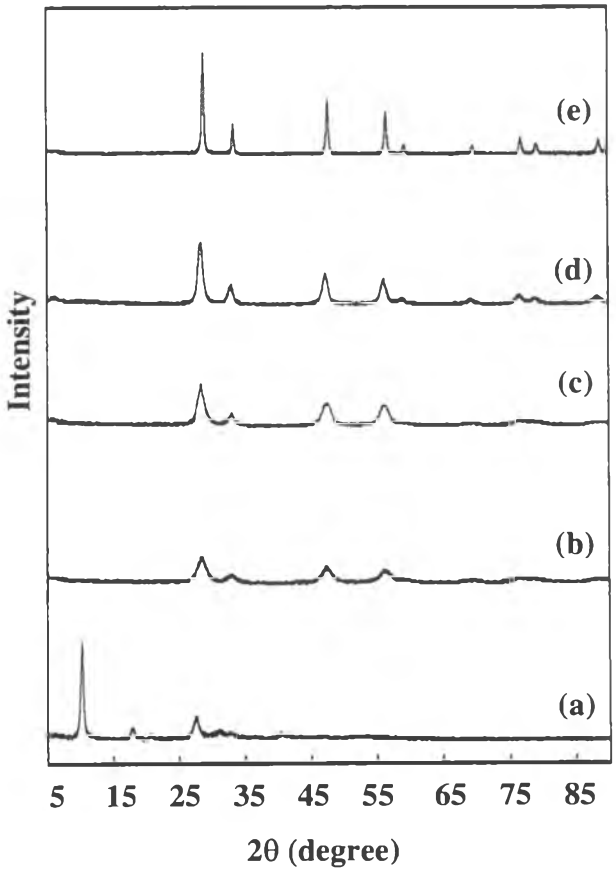

Figure 7. (Ksapabutr et al.)

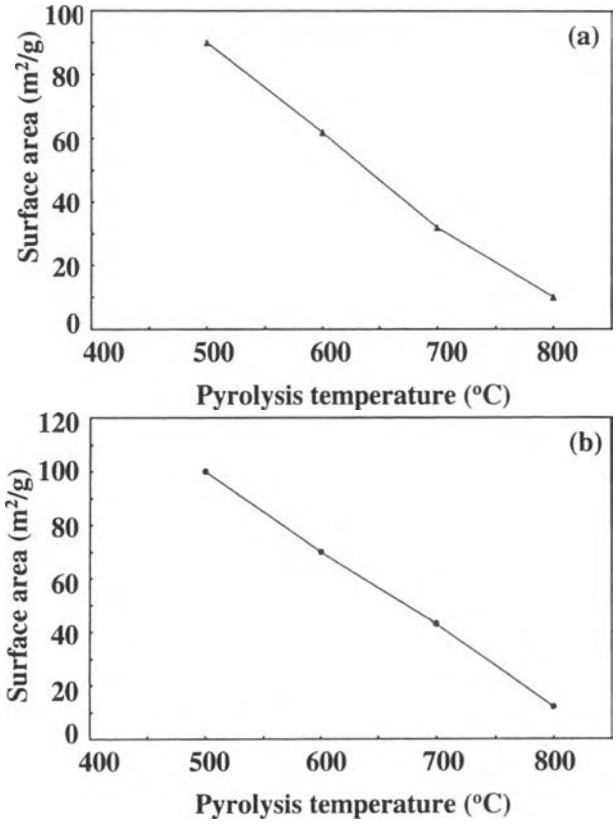

Figure 8. (Ksapabutr et al.)

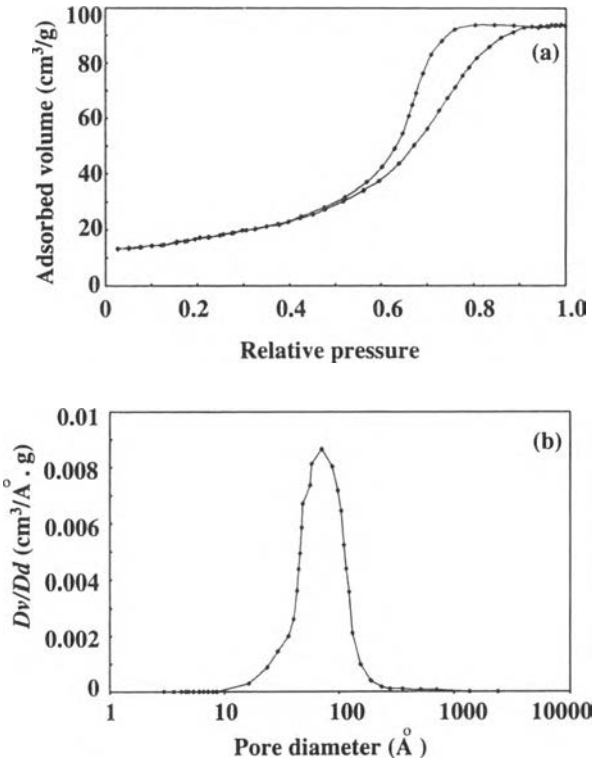

Figure 9. (Ksapabutr et al.)

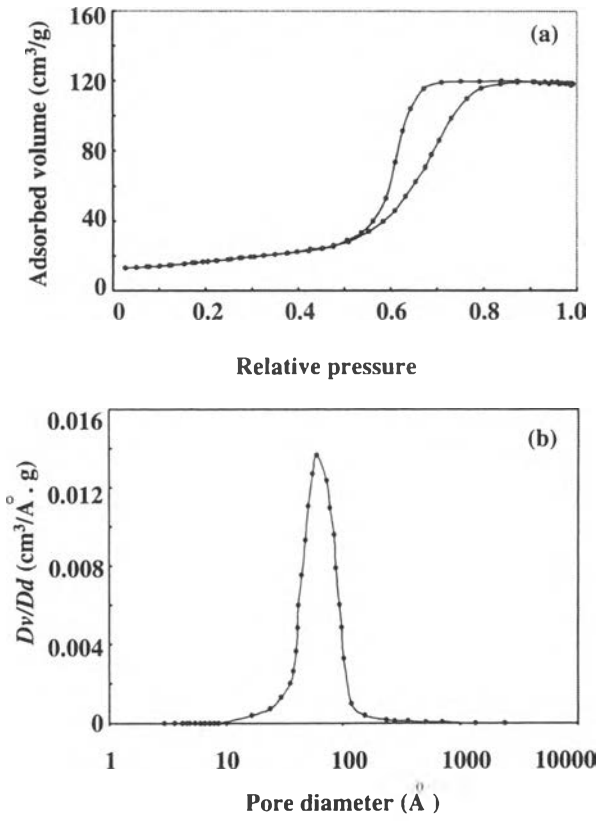

Figure 10. (Ksapabutr et al.)

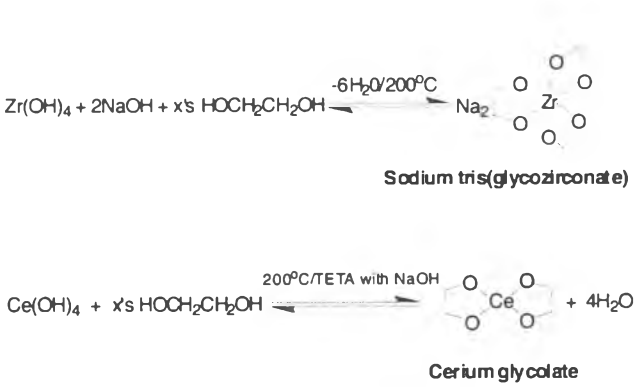

Scheme 1. (Ksapabutr et al.)

Table Captions

Table 1. Proposed structures and fragmentation pattern of sodium tris(glycozirconate) complex in crude and purified forms.

Table 2. Proposed structures and fragmentation pattern of cerium glycolate complex in crude and purified forms.

Crude product		Purified product	
m/e (% intensity)	Proposed fragment	m/e (% intensity)	Proposed fragment
635 (11.5)	$[Na_4Zr_2C_{12}H_{24}O_{12}]-H^+$	318 (30.6)	$[Na_2ZrC_6H_{12}O_6]-H^+$
583 (9.4)	$[Na_3Zr_2C_{11}H_{22}O_{11}]-2H^+$	297 (87.6)	$[NaZrC_6H_{12}O_6]-3H^+$
543 (27.2)	$[Na_2Zr_2C_{11}H_{22}O_{10}]-H^+$	258 (33.7)	$[ZrC_6H_{12}O_5]-3H^+$
498 (45.3)	$[Na_2Zr_2C_9H_{18}O_9]^+$	225 (56.2)	$[ZrC_5H_{10}O_4]^+$
469 (38.7)	$[Na_2Zr_2C_8H_{16}O_8]-H^+$	182 (100.0)	$[ZrC_3H_6O_3]-H^+$
318 (24.2)	$[Na_2ZrC_6H_{12}O_6]-H^+$	151 (39.9)	$[ZrC_2H_4O_2]^+$
297 (48.7)	$[NaZrC_6H_{12}O_6]-3H^+$		
257 (22.6)	$[ZrC_6H_{12}O_5]-2H^+$		
225 (15.1)	$[ZrC_5H_{10}O_4]^+$		
182 (61.1)	$[ZrC_3H_6O_3]-H^+$		
151 (80.7)	$[ZrC_2H_4O_2]^+$		
122 (33.4)	$[ZrCH_2O]-H^+$		

Table 1. (Bussarin et al.)

Crude product		Purified product	
m/e (% intensity)	Proposed fragment	m/e (% intensity)	Proposed fragment
783 (17.11)	$[Ce_3C_{12}H_{24}O_{12}]-3H^+$	262 (14.67)	$[CeC_4H_8O_4]-2H^+$
753 (10.17)	$[Ce_3C_{11}H_{22}O_{11}]-3H^+$	244 (5.90)	$[CeC_4H_8O_3]^+$
705 (39.23)	$[Ce_3C_{10}H_{20}O_9]-H^+$	184 (100)	$[CeC_2H_4O]^+$
521 (11.75)	$[Ce_2C_8H_{16}O_8]-H^+$	170 (24.01)	$[CeCH_2O]^+$
504 (9.26)	$[Ce_2C_8H_{16}O_7]^+$	156 (0.10)	$[CeO]^+$
445 (21.32)	$[Ce_2C_6H_{12}O_5]-H^+$		
430 (16.93)	$[Ce_2C_5H_{10}O_5]^+$		
261 (24.27)	$[CeC_4H_8O_4]-H^+$		
244 (8.92)	$[CeC_4H_8O_3]^+$		
184 (70.5)	$[CeC_2H_4O]^+$		
170 (42.15)	$[CeCH_2O]^+$		
156 (2.33)	$[CeO]^+$		

Table 2. (Bussarin et al.)